



Universiteit
Leiden
The Netherlands

Identification of novel targets in prostate cancer progression

Ghotra, V.P.S.

Citation

Ghotra, V. P. S. (2013, December 19). *Identification of novel targets in prostate cancer progression*. Retrieved from <https://hdl.handle.net/1887/22947>

Version: Corrected Publisher's Version

License: [Licence agreement concerning inclusion of doctoral thesis in the Institutional Repository of the University of Leiden](#)

Downloaded from: <https://hdl.handle.net/1887/22947>

Note: To cite this publication please use the final published version (if applicable).

Cover Page



Universiteit Leiden



The handle <http://hdl.handle.net/1887/22947> holds various files of this Leiden University dissertation

Author: Ghotra, Veerander Paul Singh

Title: Identification of novel targets in prostate cancer progression

Issue Date: 2013-12-19

CHAPTER 5

IN VIVO RNAI IDENTIFIES SYK AS A CANDIDATE DRUG TARGET FOR PROSTATE CANCER

Veerander PS Ghotra ¹, Shuning He ², Geertje van der Horst ³, Steffen Nijhoff ⁴, Hans de Bont ¹, Annemarie Lekkerkerker ⁴, Richard Janssen ⁴, Gabri van der Pluijm³, Guido Jenster ⁵, Geert JLH van Leenders ⁶, A. Marije Hoogland ⁶, Zuzanna Baranski ¹, Bob van de Water ¹, B. Ewa Snaar-Jagalska ² and Erik HJ Danen ¹

Submitted

¹Division of Toxicology, Leiden Academic Center for Drug Research and ²Department of Molecular cell Biology, Institute of Biology, Leiden University, Leiden, the Netherlands; ³Division of Urology, Leiden University Medical Center, Leiden, The Netherlands; ⁴Galapagos BV, Leiden, The Netherlands; ⁵Department of Urology and ⁶Department of Pathology, Erasmus University Medical Center, Rotterdam, The Netherlands

ABSTRACT

In an adenoviral RNAi screen using a zebrafish xenograft automated bioimaging platform (1), we identify SYK as a kinase supporting human prostate cancer dissemination. SYK has not been previously implicated in prostate cancer and we confirm SYK mRNA and protein expression in human prostate cancer specimens. Stable lentiviral silencing confirms a role for SYK in zebrafish xenografts and demonstrates that SYK supports in vitro invasive outgrowth of prostate cancer spheroids. In a mouse experimental prostate cancer metastasis model, SYK RNAi prevents bone colonization and this effect is reversed by wild type but not kinase dead SYK expression. In absence of SYK, cell surface expression of the progression-associated adhesion receptors, integrin alpha-2 and CD44 is diminished and silencing alpha-2 phenocopies SYK depletion in vitro and in vivo. Finally, pharmacological inactivation of SYK similarly interferes with invasive growth and dissemination. As SYK inhibitors are already in Phase I-II clinical trials for rheumatoid arthritis and lymphoid malignancies (2, 3), these preclinical findings can be immediately translated to the clinic to assess efficacy in the treatment of prostate cancer.

INTRODUCTION

Prostate cancer is the most common cancer in males and the second leading cause of cancer deaths among men in the Western world (4). Non-detectable micro-metastatic disease may be present in up to 40% of patients (5) while 8–14% may have visible or symptomatic bone metastases at diagnosis (6). Although the majority of prostate cancers are diagnosed as organ-confined disease, which is curable by prostatectomy or radiation therapy, 20–25% of patients will experience relapse within 5 years of treatment (7). Once the disease has spread beyond the prostate, no curative treatments are currently available (8). In addition to screening programs for early diagnosis and treatment of localized disease, there is an urgent need for novel targeted therapies to improve treatment of metastatic prostate cancer.

RESULTS AND DISCUSSION

A panel of prostate cancer cell lines was xenografted in the yolk of zebrafish and dissemination was analyzed using a whole animal automated bioimaging platform as described (1). Prostate cancer cell lines reported to be androgen-independent and/or metastatic in mice (LNCaP-derived C4-2 and C4-2B; DU145 and PC3) showed enhanced dissemination in comparison with androgen-dependent non-metastatic cells (LNCaP) (9–12) (Fig S1). We therefore devised an adenovirus-based RNAi screen for mediators of prostate cancer dissemination using this platform (Fig 1a). Two independent shRNAs targeting the protein tyrosine kinase, SYK were identified that significantly inhibited PC3 spreading in two independent experiments using ~25 embryos per condition (Fig 1b,c; Fig S2). Additional genes fulfilling these criteria included the cell surface hyaluronan receptor, CD44 and the tyrosine kinase, Src (Fig 1b) that have already been linked to growth and progression of prostate cancer (13–16).

SYK has been extensively implicated in lymphoid malignancies (3) and appears to play opposing roles in different solid tumors (17, 18) but has not been previously associated with prostate cancer. Two independent lentiviral SYK shRNAs confirmed the role of SYK in dissemination in the zebrafish xenograft model (Fig 1d; Fig S3). SYK RNAi also appeared to reduce outgrowth of cells at the primary injection site (Fig S2) and SYK-depleted PC3 cells showed impaired colony formation capacity in vitro (Fig 1e). Moreover, in a model

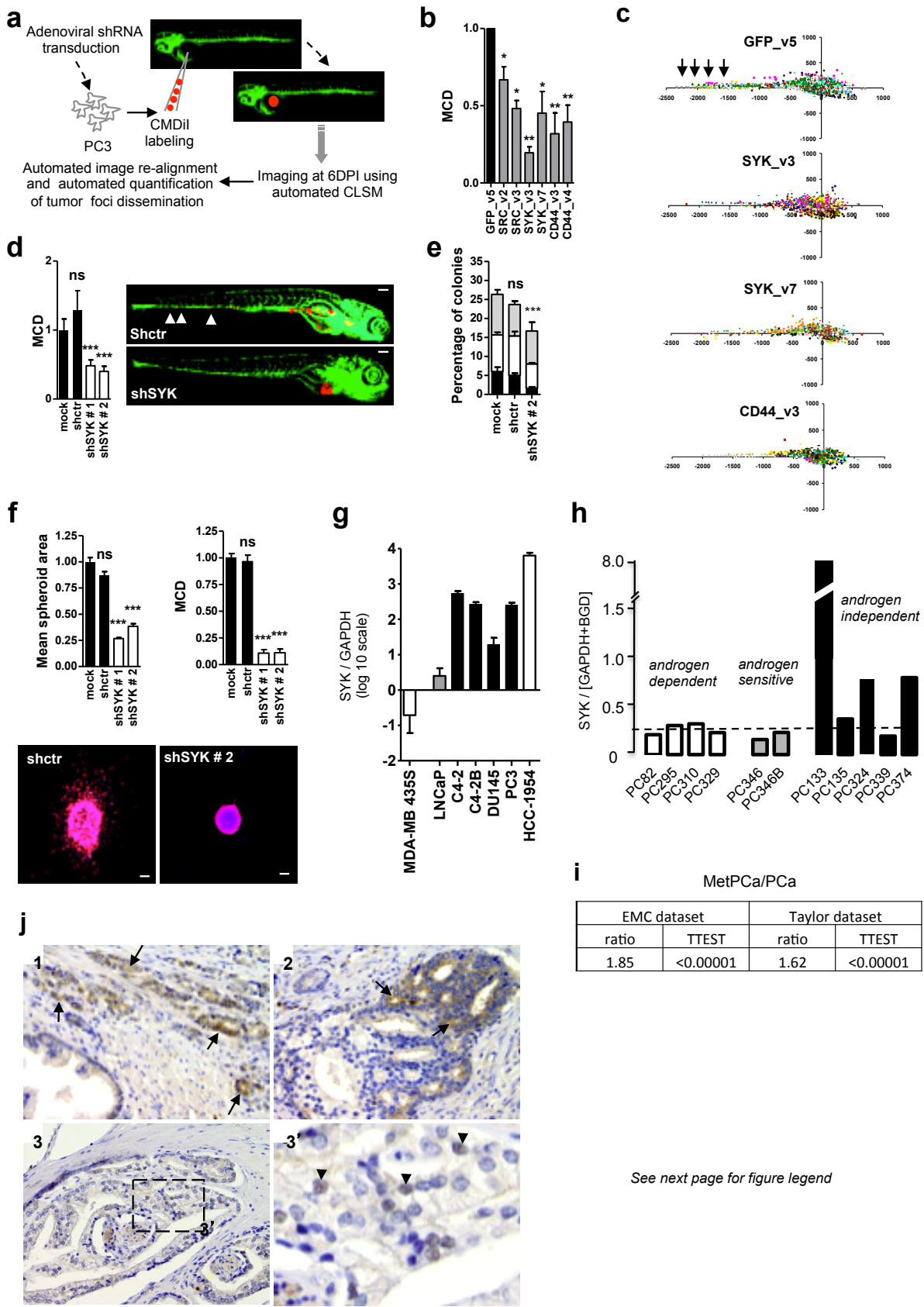


Figure 1

See next page for figure legend

FIGURE 1. *SYK is expressed in human prostate cancer and supports growth, invasion, and dissemination of prostate cancer cells.* (a) Schematic overview of the in-vivo screening procedure. (b) Mean cumulative distance (MCD) of tumor foci relative to site of injection for PC3 cells transiently transduced with indicated adenoviral shRNAs calculated from >40 xenografts obtained from two independent experiments. (c) Representative scatter plots showing tumor foci detected by automated confocal imaging and automated image analysis as described (1) in zebrafish injected with PC3 cells expressing indicated adenoviral shRNAs. Each color shows foci detected in one embryo. Arrows indicate foci in tail region. (d) MCD and representative images for dissemination in zebrafish of PC3 cells stably expressing indicated lentiviral SYK shRNAs (combined data from 2 independent experiments using >32 embryos per condition are shown). (e) Quantification of colony formation assay for PC3 cells expressing indicated lentiviral SYK shRNAs. Grey, small; white, medium; black, large colonies. (f) Representative images and quantification of expansion (mean spheroid area) and ECM invasion (MCD) for control and shSYK PC3 cell spheroids 6 days post-injection in collagen gels (blue, Hoechst; red, Phalloidin). Scale bars, 100 μ m. (g) SYK RNA expression determined by qPCR in indicated cell lines. MDA-MB-435S (hypermethylated SYK gene promoter (35, 36)) and HCC-1954 breast cancer cells (high SYK expression (36)) were used as negative and positive controls, respectively. (h) SYK RNA expression in human prostate cancer resection specimens xenografted in mice. (i) Ratio between SYK RNA expression in prostate cancer metastases (MetPCa) and primary prostate cancers (PCa) and significance (TTEST) in two different datasets. (j) Immunohistochemical staining of SYK protein in three different prostate cancer specimens (1-3). Arrows point to cytoplasmic staining in cancer cells. Arrowheads in enlargement 3' point to infrequently observed nuclear staining. ns, not significant; * p <0.05; ** p <0.01; *** p <0.005.

where cell spheroids are embedded in three dimensional (3D) extracellular matrix (ECM) scaffolds (19), silencing SYK attenuated spheroid expansion and effectively blocked ECM invasion (Fig 1f; Fig S4; Video S1). No signs of increased nuclear fragmentation in SYK-depleted spheroids were observed, pointing to decreased proliferation rather than cell death as the underlying mechanism (Fig S4).

We next analyzed SYK expression in human prostate cancer. Compared to LNCaP, mRNA expression was increased in the androgen-independent LNCaP-derived C4-2 and C4-2B sublines and in DU145 and PC3 androgen-independent, metastatic prostate cancer cell lines (Fig 1g). Likewise, in a series of human prostate cancer xenografts (20), SYK mRNA expression was higher in androgen-independent tumors (Fig 1h) and SYK expression in prostate cancer metastasis resection specimens was significantly increased compared to primary prostate cancer in two datasets (Fig 1i). Since the stromal compartment may affect mRNA analysis in clinical samples, SYK protein expression was analyzed in a set of primary prostate cancer specimens. Immunohistochemistry validated SYK expression in prostate cancer cells and expression was increased in prostate cancer versus normal prostate epithelium (Fig 1j).

In acute lymphoid leukemia (AML), inhibition of SYK promotes differentiation (21). We analyzed a set of transcripts previously associated with undifferentiated characteristics of prostate cancer cells (22) but observed no gross changes in the expression of these genes upon depletion of SYK. However, while mRNA levels of the prostate cancer progression-associated markers CD44 and integrin α 2 β 1 (13, 14, 23-25) were unaffected (Fig S5); their cell surface expression was lost following SYK depletion (Fig 2a). SYK has been previously reported to regulate surface expression of transmembrane receptors (26, 27) and two adenoviral CD44 shRNAs were identified as hits in our primary screen (Fig 1b). Moreover, lentiviral silencing of α 2 or β 1 integrin subunits, each by two independent shRNAs, suppressed 3D ECM invasion as well as dissemination in the zebrafish model (Fig 2b,c; Fig S6). A role for β 1 integrins in intravascular locomotion of tumor cells in zebrafish has been previously reported (28). Together, these results identify regulation of surface expression of adhesion receptors as a potential underlying mechanism for the support of prostate cancer dissemination by SYK.

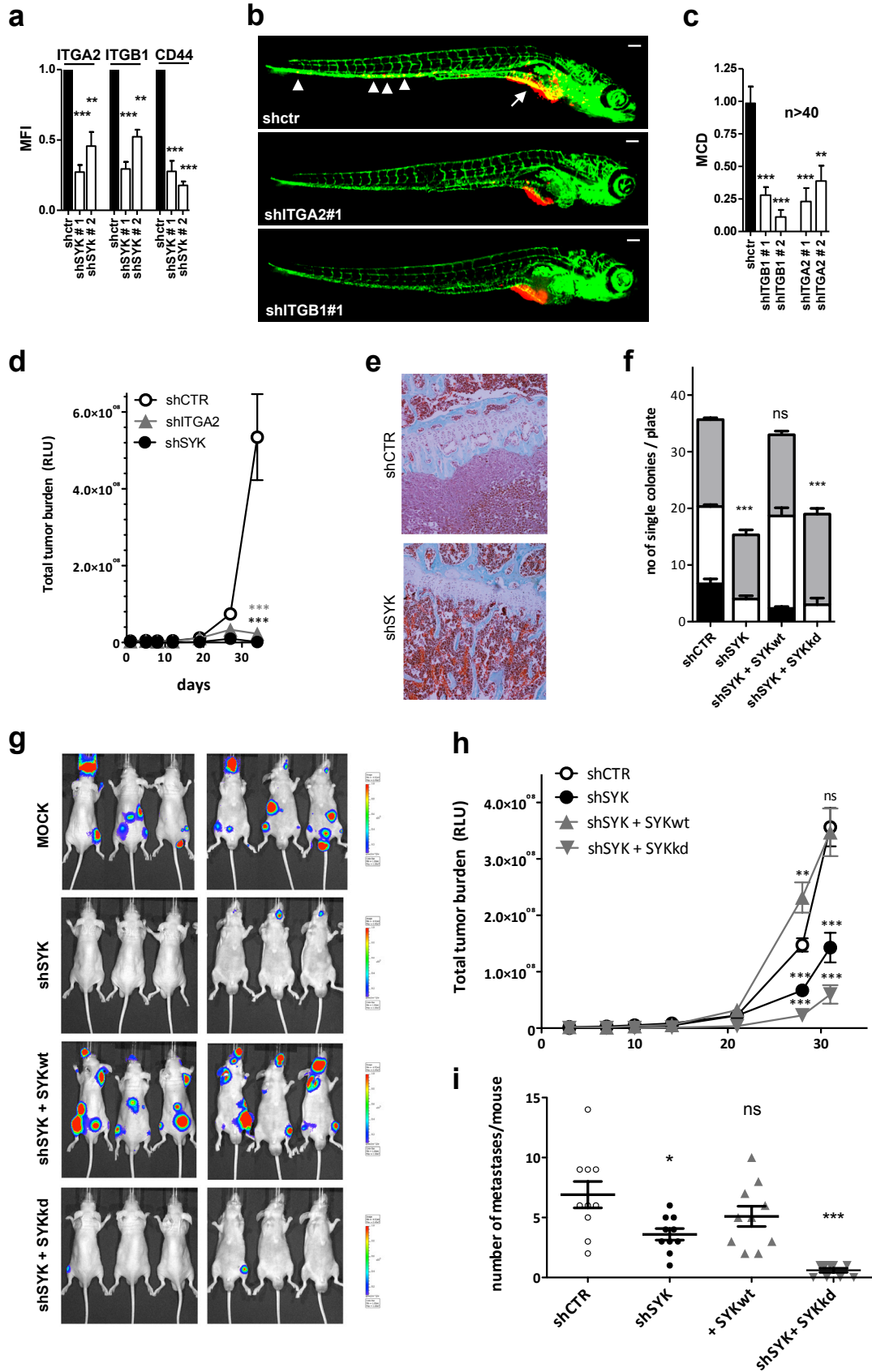


Figure 2. See next page for figure legend

FIGURE 2. SYK regulation of adhesion receptor surface expression in human prostate cancer cells modulates dissemination in zebrafish and metastatic colonization in mice. (a) FACS analysis of surface expression of CD44 and integrin subunits $\alpha 2$ (ITGA2) and $\beta 1$ (ITGB1) in PC3 cells expressing indicated SYK shRNAs. MFI, mean fluorescence intensity. (b,c) Representative images (b) and quantified MCD (c) for dissemination in zebrafish of PC3 cells expressing indicated lentiviral shRNAs (combined data from 2 independent experiments using > 40 embryo's per condition are shown; Scale bar is 100 μ m). Arrow heads indicate tumor foci in tail region. (d) Total metastatic tumor burden determined by BLI monitoring at indicated time points following intra-cardiac inoculation in immune-compromised mice for PC3M-Pro4luc variants expressing indicated lentiviral shRNAs (data obtained from at least 9 mice per experimental group). (e) Bones of mice collected 31 days after intracardiac inoculation with PC3M-Pro4-luc shCTR or shSYK cells and stained with Goldner staining. *, tumor lesion. (f) Quantification of colony formation assay for PC3M-Pro4-luc cells expressing control or SYK shRNAs in combination with wild type (SYKwt) or kinase dead SYK (SYKkd) expression vectors. Grey, small; white, medium; black, large colonies. (g) BLI images of PC3M-Pro4luc variants expressing control or SYK shRNAs in combination with wild type (SYKwt) or kinase dead (SYKkd) expression vectors taken 31 days following intra-cardiac inoculation. (h,i) Quantification of the experiment shown in (g) where total metastatic tumor burden was determined by BLI monitoring at indicated time points (h) and the number of metastatic colonies was determined by counting of BLI foci at 31 days following intra-cardiac inoculation (data obtained from at least 10 mice per experimental group) (i). ns, non significant; * $p < 0.05$; ** $p < 0.01$; *** $p < 0.005$ versus shCTR.

We next addressed the role of SYK in a preclinical mouse xenograft model for prostate cancer bone metastasis (29). Depletion of SYK led to a strong reduction in metastatic tumor burden following intracardiac inoculation of PC3M-Pro4luc cells (Fig 2d,e). Similar to its effect in vitro and in zebrafish xenografts; shRNA targeting integrin 2-subunit mRNA, phenocopied shSYK in this model (Fig 2d). To further interrogate the specific role for SYK kinase activity in prostate cancer bone colonization, wild type or kinase dead SYK was expressed in PC3M-Pro4luc cells expressing an shRNA targeting the SYK 3'UTR. Wild type but not kinase dead SYK rescued the in vitro colony forming ability of these cells (Fig 2f). Moreover, effective bone colonization of shSYK cells was restored by wild type SYK while expression of kinase dead SYK even further suppressed the process with very few detectable metastases (Fig 2g-i).

Based on these findings, we performed initial experiments to evaluate whether pharmacological inhibition of SYK could interfere with in vitro invasive outgrowth and in vivo dissemination using zebrafish xenografts. Small molecule inhibitors of SYK are in clinical development for autoimmune diseases and lymphoid malignancies (2, 3). Two of these compounds, R-406 and BAY-61-3606 show efficacy in preclinical leukemia and retinoblastoma studies (21, 30-33). When used at 1-10 μ M, the concentration widely used in vitro (21, 30-33) these compounds reduced spheroid outgrowth and ECM invasion of PC3 as well as C4-2B cells (Fig 3a-c). Moreover, R-406 significantly inhibited dissemination of PC3 cells (Fig 3d) without significant signs of toxicity at 10 μ M (e.g. yolk sac edema, cardiac edema, bending of the tail, hepatic necrosis, and impaired cardiovascular function were compared for R-406 and vehicle control treated animals). Thus, pharmacological inactivation of SYK using R-406 and BAY-61-3606 recapitulated the effect of silencing the SYK gene in vitro and in zebrafish xenografts.

In summary, we demonstrate that a semi-automated whole animal bioimaging assay based on zebrafish xenotransplantation (1) can be productive in RNAi-based preclinical target discovery and lead compound identification. We show that genetic and pharmacological inactivation points to a role for SYK in invasive growth and dissemination of prostate cancer. SYK mRNA and protein is detected in human prostate cancer tissues and SYK inhibitors have already been tested in phase I-II clinical trials for other diseases. Altogether, this establishes SYK as a potential new drug target in prostate cancer for which existing pharmacological inhibitors with known toxicological profiles can be tested for clinical efficacy.

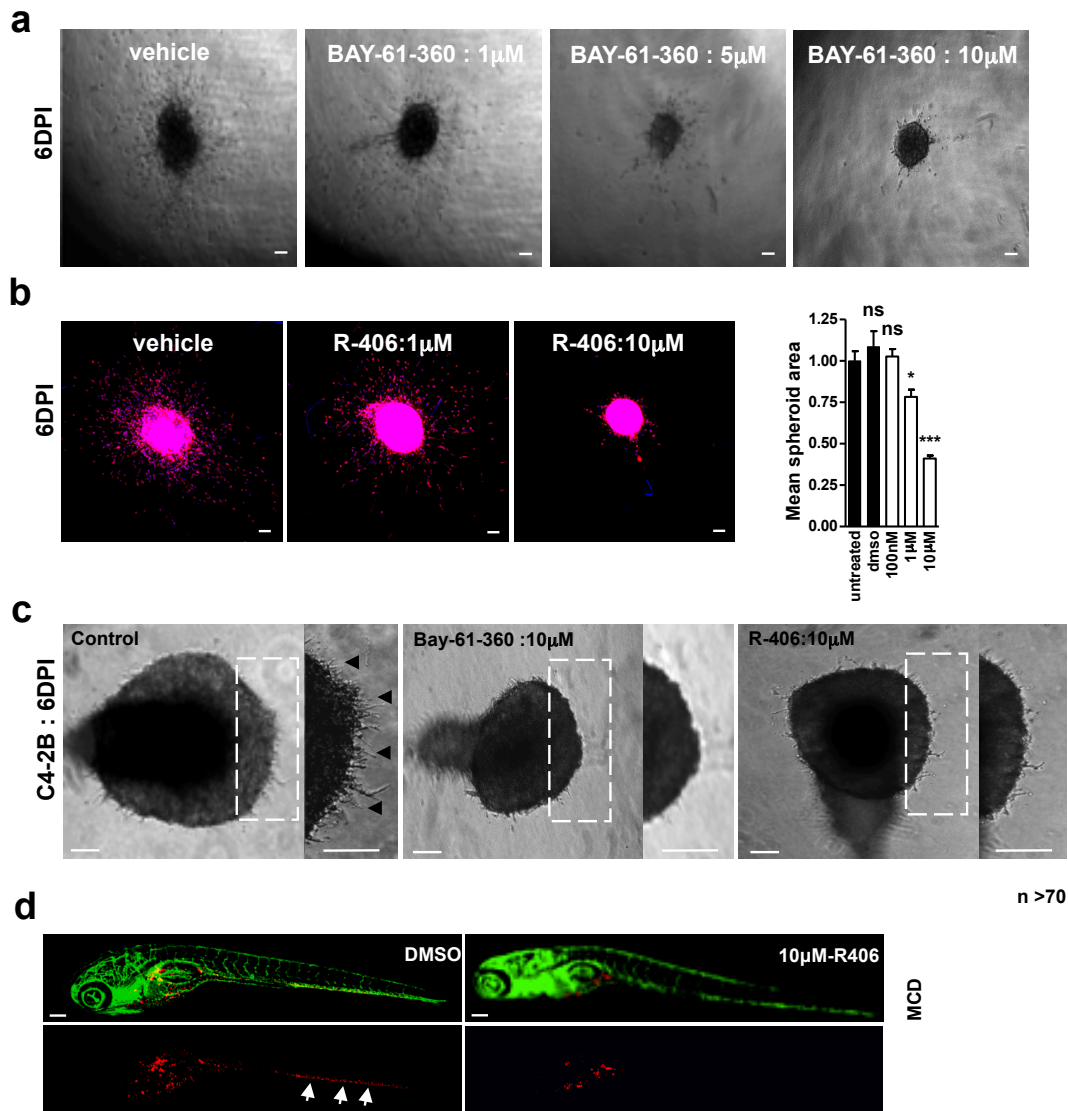


FIGURE 3. *Pharmacological inhibition of SYK prevents growth, invasion, and dissemination of prostate cancer cells.* (a) Bright field images showing PC3 spheroids 6 days post-injection into collagen gels in the absence or presence of the indicated concentrations of BAY-61-360 (one of three experiments is shown). (b) Representative images and quantification of expansion (mean spheroid area) and ECM invasion (MCD) for PC3 cell spheroids measured at 6 days post-injection in collagen gels and treated with indicated concentrations of R-406 (blue, Hoechst; red, Phalloidin; scale bar is 120 μ m). (c) Brightfield images showing C4-2B cell spheroids at 6 days post formation in the absence or presence of the indicated concentrations of SYK inhibitors. Arrowheads point to ECM invading strands seen under control conditions, which are not observed in presence of inhibitors. Scale bar is 120 μ m. (d) Representative images and quantified MCD for dissemination in zebrafish of PC3 cells in the absence or presence of indicated concentrations of R-406. Combined data from 2 independent experiments using >70 embryos per condition are shown. Arrows point to cells disseminated to tail region. Scale bar is 100 μ m; ns, not significant; *p<0.05; ** p<0.01; ***p<0.005.

METHODS

See supplemental information for detailed Materials and Methods.

LNCaP, PC3 and DU-145 cells were obtained from ATCC and cultured according to the provided protocol. PC3M-Pro4luc cells have been described previously (29). LNCaP-derived cell lines C4-2 and C4-2 B were grown in T-Medium. Zebrafish embryo xenografting followed by automated confocal imaging and image analysis algorithms were previously described (1). Dissemination is described as cumulative distance from injection site of tumor cells in each embryo averaged over all embryos (mean cumulative distance; MCD). For the shRNA screen, PC3 cells were transduced with adenoviral shRNA constructs 5 days prior to xenotransplantation. Stable PC3 and PC3M-Pro4-luc cell lines were generated by lentiviral shRNA (TRC; Sigma) transduction followed by bulk puromycin selection. Wild type or kinase dead (K402R) SYK retrovirus (34) (a kind gift from Drs. Wei Zou and Steven Teitelbaum, Washington University, St Louis MO) was transduced in PC3M-Pro4-luc cells stably expressing shRNA targeting the SYK 3'UTR, followed by bulk blasticydin selection. RNA isolation, qPCR, immunohistochemistry on paraffin-embedded tissues, and FACS were done using standard protocols. Growth and ECM invasion was studied for cell spheroids embedded in collagen gels as described (19) and quantified using an automated Image pro 7-based plugin to calculate surface area of spheroid, number of cells migrating out and cumulative distance travelled by these cells. The latter is described as MCD. Experimental bone metastasis in mice was analyzed by weekly whole body bioluminescent imaging (BLI) and Goldner bone staining in nude mice following intracardiac injection with PC3M-Pro4luc cells as described (29). Data for all experiments are presented as mean \pm SEM of at least 3 independent biological replicates unless otherwise stated. Student's t test (two-tailed) was used to compare groups.

ACKNOWLEDGEMENTS

We thank Drs Wei Zou and Steven Teitelbaum for kindly providing SYK plasmids. This work was supported by grants from EU FP7 (HEALTH-F2-2008-201439) and Dutch Cancer Society (UL-2010-4670).

AUTHOR CONTRIBUTIONS

V.P.S.G., S.H.G.v.d.H., S.N.H.d.B., A.M.H., A.L., Z.B., and E.H.J.D. designed and performed experiments. R.J., G.v.d.P., G.J., G.J.L.H.v.L., B.v.d.W., B.E.S.-J., and E.H.J.D. analyzed and interpreted data. V.P.S.G. and E.H.J.D. wrote the manuscript.

SUPPLEMENTARY INFORMATION : METHODS

Cell lines and antibodies

LNCaP, PC3 and DU-145 cells were obtained from ATCC and cultured according to the provided protocol. PC3-M-Pro4luc cells have been described previously (1). LNCaP-derived cell lines C4-2 and C4-2B were grown in T-Medium. For FACS, primary antibodies included AIIB2 anti-human integrin β 1, 4A10 anti human integrin α 2, and sc-18849 anti-human CD44 (Santa-Cruz). Goat-anti-mouse APC and donkey-anti-rat PE (Jackson laboratories) were used as secondary antibodies. For immunohistochemistry in patient tumor samples Syk N-19 Ab (sc-1077; Santa Cruz) was used.

Zebrafish xenotransplantation experiments

For quantification of tumor cell spreading, tumor cells were labeled with CM-Dil (Invitrogen), mixed with 2% PVP, and injected into the yolk sac of enzymatically dechorionated, two-day old Casper fli-EGFP transgenic zebrafish embryos using an air driven microinjector (20 psi, PV820 Pneumatic PicoPump; World precision Inc). Embryos were maintained in egg water at 34°C for 6 days and subsequently fixed with 4% paraformaldehyde. Imaging was done in 96 well plates containing a single embryo per well using a Nikon Eclipse Ti confocal laser-scanning microscope. Z stacks (12 x 30 μ m) were obtained using a Plan Apo 4X Nikon dry objective with 0.2 NA and 20 WD. Images were converted into a single Z projection in Image-Pro Plus (Version 6.2; Media Cybernetics). Automated quantification of cumulative tumor cell spreading per embryo was carried out using an in-house built Image-Pro Plus plugin as previously described (2).

Transient adenoviral shRNA transduction

PC3 cells were transduced one day after seeding with adenoviral shRNA constructs from Galapagos BV (Leiden, the Netherlands) using an MOI of 15 for 24 h. After 3 days, medium was replaced and after an additional two days, the transduced PC3 cells were detached with trypsin and single cell suspensions were used for zebrafish xenotransplantation.

Stable shRNA and cDNA expression

PC3 or PC3-M-Pro4luc cells were transduced using Sigma's MISSION library lentiviral shRNAs (shSYK#1: TRCN0000003167, shSYK#2: TRCN0000199566; shITGB1#1: TRCN0000029645, shITGB1#2: TRCN0000029646; shITGA2#1: TRCN0000057730, shITGA2#2: TRCN0000057731). For lentivirus production, HEK293T cells were transfected with the short hairpin constructs together with the packaging plasmids REV, GAG and VSV in a 1:1:1:1 ratio using PE (Sigma) as transfection reagent. Lentiviral supernatant was collected 48 h after transfection and used for transduction or target cells in the presence of 8 μ g Polybrene (Sigma). Transduced cells were bulk selected in medium containing 2 μ g/ml puromycin. Lentiviral shRNA vector targeting TurboGFP was used as a negative control. Retroviral cDNAs for wild type and kinase dead SYK were a gift from Drs. Wei Zou and Steven Teitelbaum, Washington University, St Louis MO (3). Retrovirus was produced in Plat-E packaging cells and used for transduction of PC3-M-Pro4-luc cells stably expressing shRNA targeting SYK 3'UTR, followed by bulk blasticidin selection.

mRNA expression analysis

For qPCR, total RNA was extracted using RNA easy Plus Mini Kit (Qiagen). cDNA was randomly primed from 50 ng total RNA using iScript cDNA synthesis kit (BioRad) and real-time qPCR was subsequently performed in triplicate using SYBR green PCR (Applied Biosystems) on a 7900HT fast real-time PCR system (Applied Biosystems).

The following qPCR primer sets were used:

GAPDH: forward AGCCACATCGCTCAGACACC,	reverse ACCCGTTGACTCCGACCTT;
SYK forward GATGCTGGTTATGGAGATG,	reverse TCTATGATGTTCTTATCCTTGAC;
CD44 forward TGGCACCCGCTATGTCCAG,	reverse GTAGCAGGGATTCTGTCTG;
ITGB1 forward ATTGACCTCTACTACCTT,	reverse GTGTTGTGCTAATGTAAG;
ITGA2 forward AACTCTTTGGATTTGCGTGTG,	reverse TGGCAGTCTCAGAATAGGCTTC.

Data were collected and analyzed using SDS2.3 software (Applied Biosystems). Relative mRNA levels after correction for GAPDH control mRNA, were expressed using $2^{(-\Delta\Delta Ct)}$ method. For mRNA expression analysis of human prostate cancer patient material either directly or following xenografting in mice, existing data-sets were queried as described (4).

Colony-Forming Assay

Cells were seeded into a 96-well plate containing ~1 cell per well. After 1 to 3 weeks, percentage of wells showing colonies and colony size was determined by microscopy (Zeiss Axiovert 200M).

3D invasion assays

Cell suspensions in PBS containing 2% polyvinylpyrrolidone (PVP; Sigma-Aldrich) were microinjected (~1x10⁴ cells/droplet) using an air driven microinjector (20 psi, PV820 Pneumatic PicoPump; World precision Inc) into solidified 3D collagen gels in 8 well μ slides (IBIDI) as previously described (5). Collagen gels were prepared from 2.5 mg/ml acid-extracted rat tail collagen type 1. Collagen was diluted to working concentration of 1 mg/ml in complete medium containing 44 mM NaHCO₃ (stock 440 mM, Merck) and 0.1 M HEPES (stock 1M, BioSolve). Tumor cell spheroids were monitored for ~1 week using Nikon eclipse TS100. For immunostaining, gels were incubated for 1 hour with 5 μ g/ml collagenase (Clostridium histolyticum, Boehringer Mannheim) at room temperature, fixed with 4% paraformaldehyde, and permeabilized in 0.2% Triton X-100. After fixation, collagen gels were stained using a cocktail containing 4 % paraformaldehyde, 0.2% Triton X-100 (Sigma) and 0.1 μ M rhodamine Phalloidin (Sigma) for 3 hrs. Thereafter, wells were washed with PBS. Preparations were then mounted in Aqua-Poly/Mount solution (Polysciences, Inc) and imaged using a Plan Apo 4X Nikon dry objective with 0.2 NA and 20 WD. A total of 15 Z planes at an interval of 30 μ m were captured. Image stacks were converted into two dimensional maximum intensity projections using Image Pro 7.0. Cell spheroids were analyzed using an automated Image pro 7-based plugin to calculate surface area of spheroid, number of cells migrating out of the cell spheroid and cumulative distance travelled by these cells.

Immunohistochemistry

Normal prostate (n=3) and primary prostate cancer specimens (n=21) were mounted on aminoacetylsilane-coated glass slides (Starfrost, Berlin, Germany), deparaffinized in xylene and dehydrated in ethanol. Endogenous peroxidase activity was blocked by 1% hydrogen peroxide in methanol for 20 min. Incubation with citrate buffer was used for antigen retrieval. Slides were incubated with 1:500 dilution of Syk antibody (sc-1077; Santa Cruz) overnight at 4°C, followed by chromogenic visualization using the EnVision DAKO kit (Dako, Glostrup, Denmark). After counterstaining with hematoxylin, slides were thoroughly washed, dehydrated, cleared in xylene and mounted in malinol (Chroma-Gesellschaft, Körgen, Germany).

Experimental bone metastasis assay

Male nude (BALB/c nu/nu) mice were anesthetized and injected with a single-cell suspension of 10⁵ cells/100 µl in PBS into the left cardiac ventricle. Outgrowth of spread PC3-M-Pro4luc cells was monitored weekly by whole body bioluminescent imaging (BLI) using an intensified charge-coupled device (I-CCD) video camera of the in vivo Imaging System (IVIS100; Xenogen, Alameda, CA, USA) as described previously (1). Values are expressed as RLU in photons/s. Bone metastases were also examined by Goldner staining after mice were sacrificed using decalcified bone.

Flow cytometry

For flowcytometry, surface expression levels were determined using primary antibodies, followed by fluorescence-conjugated secondary antibodies, and analysis on a FACSCanto or sorting on a FACS Calibur (Becton Dickinson).

Statistical analysis

Data are presented as mean ± SEM of at least 3 independent biological replicates unless otherwise stated. Student's t test (two-tailed) was used to compare groups.

References concerning methods

1. van den Hoogen, C., van der Horst, G., Cheung, H., Buijs, J.T., Pelger, R.C., and van der Pluijm, G. 2011. Integrin alphav expression is required for the acquisition of a metastatic stem/progenitor cell phenotype in human prostate cancer. *Am J Pathol* 179:2559-2568.
2. Ghotra, V.P., He, S., de Bont, H., van der Ent, W., Spaink, H.P., van de Water, B., Snaar-Jagalska, B.E., and Danen, E.H. 2012. Automated whole animal bio-imaging assay for human cancer dissemination. *PLoS One* 7:e31281.
3. Zou, W., Reeve, J.L., Zhao, H., Ross, F.P., and Teitelbaum, S.L. 2009. Syk tyrosine 317 negatively regulates osteoclast function via the ubiquitin-protein isopeptide ligase activity of Cbl. *J Biol Chem* 284:18833-18839.
4. Martens-Uzunova, E.S., Jalava, S.E., Dits, N.F., van Leenders, G.J., Moller, S., Trapman, J., Bangma, C.H., Litman, T., Visakorpi, T., and Jenster, G. 2012. Diagnostic and prognostic signatures from the small non-coding RNA transcriptome in prostate cancer. *Oncogene* 31:978-991.
5. Truong, H.H., de Sonnevile, J., Ghotra, V.P., Xiong, J., Price, L., Hogendoorn, P.C., Spaink, H.H., van de Water, B., and Danen, E.H. 2012. Automated microinjection of cell-polymer suspensions in 3D ECM scaffolds for high-throughput quantitative cancer invasion screens. *Biomaterials* 33:181-188.

SUPPLEMENTARY FIGURES

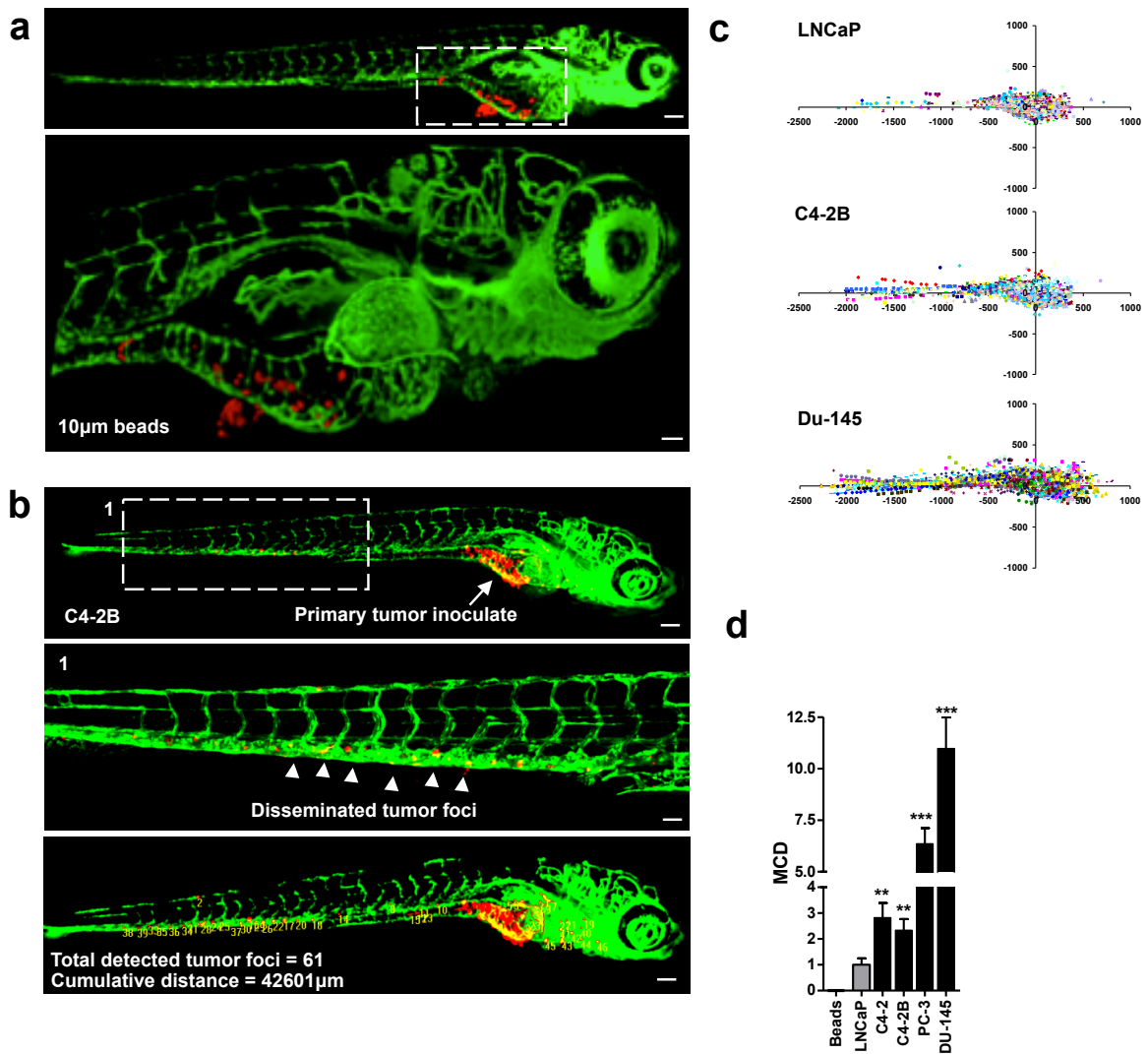


FIGURE S1. Whole organism automated bioimaging assay differentiates between androgen independent / metastatic and androgen-dependent / non-metastatic prostate cancer cells. (a) Representative image of Casper fli-EGFP embryo 6 days following yolk sac implantation of 10µm fluorescent beads. Scale bar is 100µm for upper image, and 50µm for lower enlargement of area in inset. Passive spreading of beads was virtually undetectable and used as threshold for cancer cell dissemination. (b) Representative image of C4-2B implanted embryos 6 days following xenotransplantation. Top, scale bar is 100 µm; middle, enlargement of inset, arrowheads point to disseminated tumor cells, scale bar is 50 µm; bottom, automated imaging and image analysis derived tumor foci – scale bar is 100 µm). (c) Scatter plots derived from automated imaging and image analysis of zebrafish xenografts with indicated cell lines 6 days following xenotransplantation in the yolk of Casper fli-EGFP embryos. Colors represent tumor cell foci detected in individual embryos. (d) Mean cumulative distance (MCD) determined from scatter plots in c for indicated cell lines using 10µm fluorescent beads as negative control. Data from 2 independent experiments are combined. In total 5 embryos were transplanted with beads, 128 with LNCaP, 147 with C4-2B, 147 with DU145, and 147 with PC3. ns, not significant; *p<0.05; ** p<0.01; ***p<0.005.

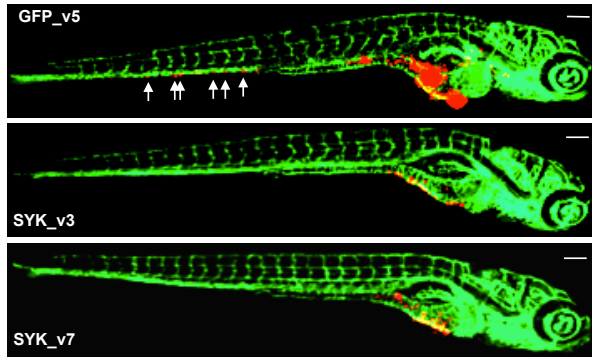


FIGURE S2. SYK depletion attenuates PC3 dissemination in zebrafish xenografts. Representative images of embryos implanted with PC3 cells expressing indicated adenoviral shRNAs at 6 days following xenotransplantation. Arrows point to tumor foci in tail region.

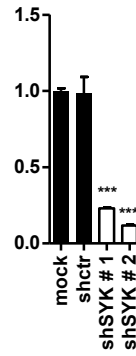


FIGURE S3. Generation of stable lentiviral bulk-puromycin selected PC3 shSYK lines. qPCR analysis of SYK expression in PC3 cells stably expressing indicated lentiviral SYK shRNAs.

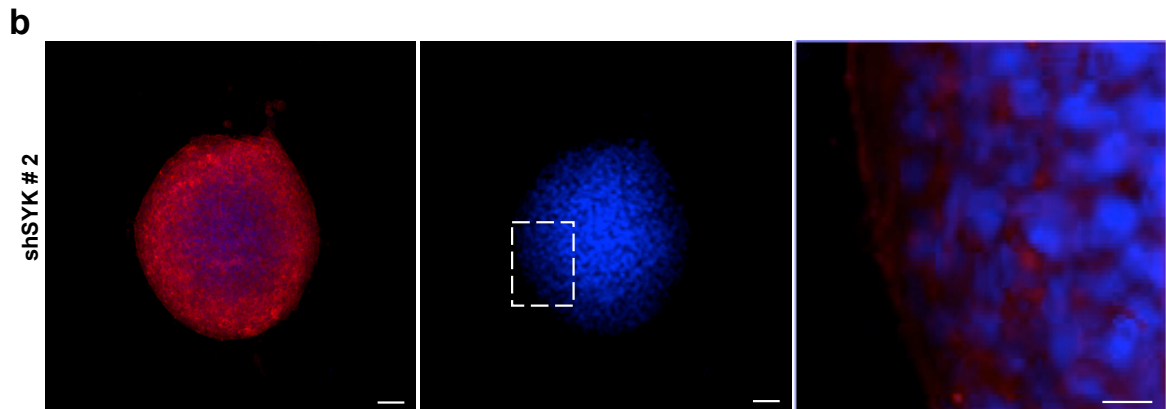
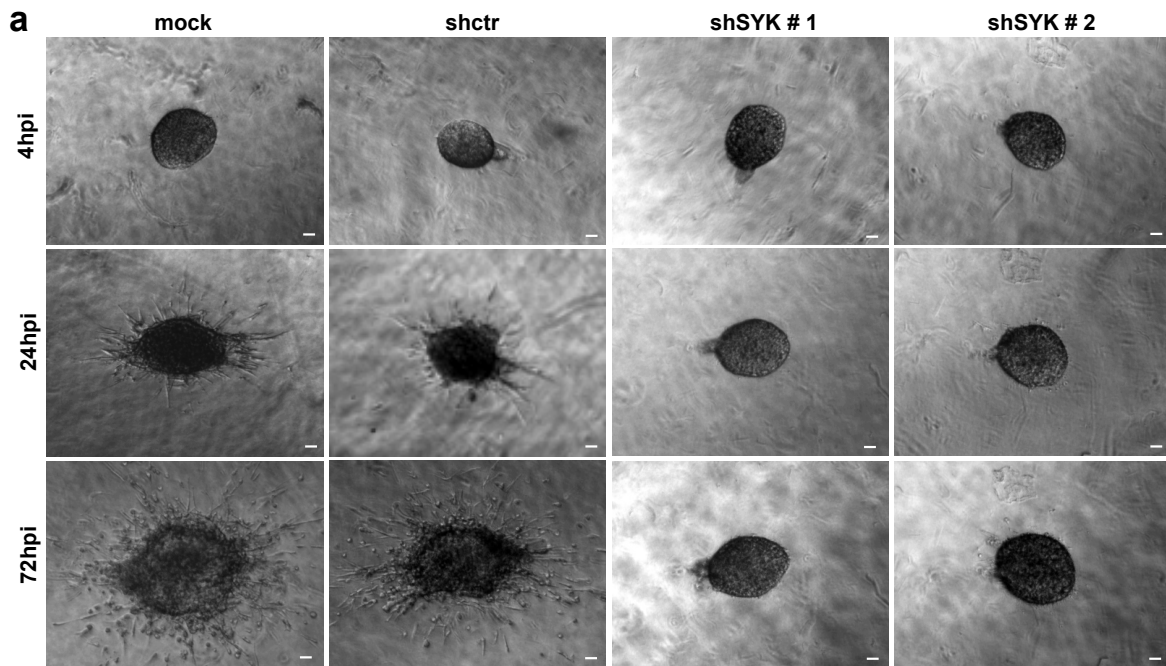


FIGURE S4. SYK depletion attenuates PC3 3D ECM invasion. (a) Bright field images showing representative spheroids of PC3 cells expressing indicated lentiviral shRNAs at 6 days post-injection into collagen gels. Scale bar is 120 μ m. (b) PC3shSYK spheroid 6 days post-formation in collagen gel, (blue, Hoechst; red, Phalloidin). Scale bars are 100 μ m.

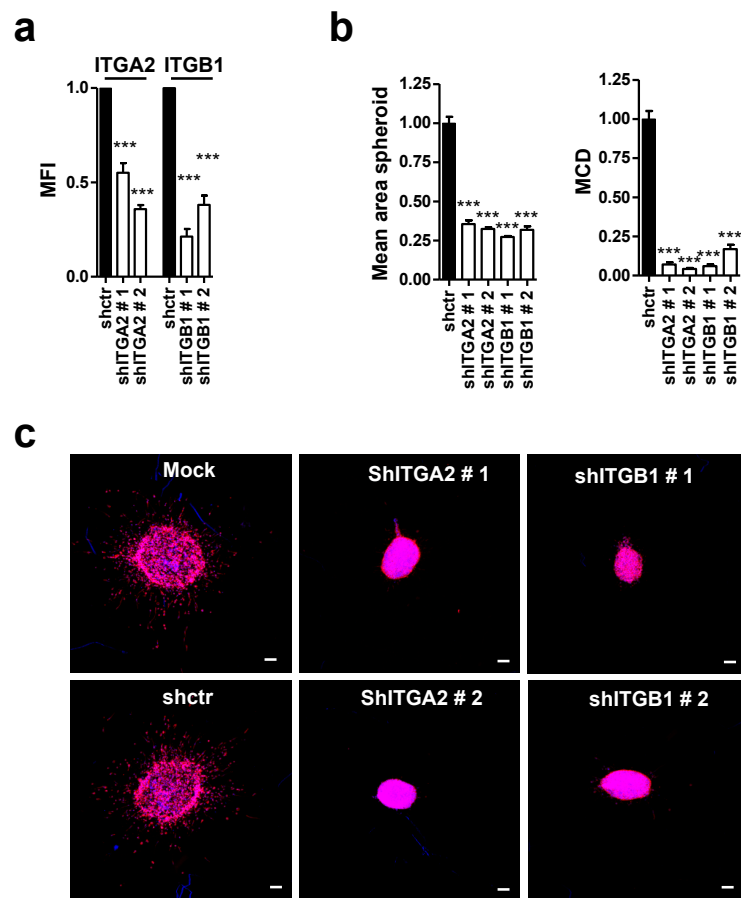
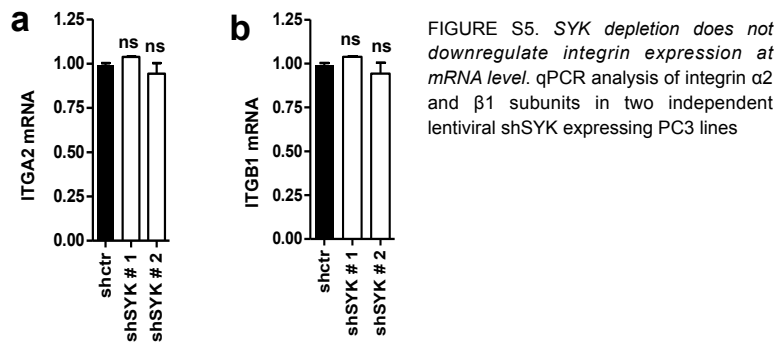


FIGURE S6. Silencing integrin $\alpha 2\beta 1$ inhibits 3D ECM invasion and outgrowth of PC3 spheroids. (a) FACS analysis of surface expression of integrin subunits $\alpha 2$ and $\beta 1$ in PC3 cells expressing lentiviral shRNAs targeting indicated integrin subunits. (b) Quantification of expansion (mean spheroid area) and ECM invasion (MCD) for cell spheroids derived from control PC3 or PC3 expressing lentiviral shRNAs targeting integrin subunits measured at 6 days post-injection in collagen gels. (c) Representative images of cell spheroids analyzed for b (blue, Hoechst; red, Phalloidin). Scale bar is 120 μ m.

REFERENCES

1. Ghotra, V.P., He, S., de Bont, H., van der Ent, W., Spaink, H.P., van de Water, B., Snaar-Jagalska, B.E., and Danen, E.H. 2012. Automated whole animal bio-imaging assay for human cancer dissemination. *PLoS One* 7:e31281.
2. Weinblatt, M.E., Kavanaugh, A., Genovese, M.C., Musser, T.K., Grossbard, E.B., and Magilavy, D.B. 2010. An oral spleen tyrosine kinase (Syk) inhibitor for rheumatoid arthritis. *The New England journal of medicine* 363:1303-1312.
3. Friedberg, J.W., Sharman, J., Sweetenham, J., Johnston, P.B., Vose, J.M., Lacasce, A., Schaefer-Cutillo, J., De Vos, S., Sinha, R., Leonard, J.P., et al. 2010. Inhibition of Syk with fostamatinib disodium has significant clinical activity in non-Hodgkin lymphoma and chronic lymphocytic leukemia. *Blood* 115:2578-2585.
4. Nelson, W.G., De Marzo, A.M., and Isaacs, W.B. 2003. Prostate cancer. *N Engl J Med* 349:366-381.
5. Freedland, S.J., Humphreys, E.B., Mangold, L.A., Eisenberger, M., Dorey, F.J., Walsh, P.C., and Partin, A.W. 2005. Risk of prostate cancer-specific mortality following biochemical recurrence after radical prostatectomy. *JAMA* 294:433-439.
6. Landis, S.H., Murray, T., Bolden, S., and Wingo, P.A. 1999. Cancer statistics, 1999. *CA Cancer J Clin* 49:8-31, 31.
7. Wirth, M.P., See, W.A., McLeod, D.G., Iversen, P., Morris, T., and Carroll, K. 2004. Bicalutamide 150 mg in addition to standard care in patients with localized or locally advanced prostate cancer: results from the second analysis of the early prostate cancer program at median followup of 5.4 years. *J Urol* 172:1865-1870.
8. Mundy, G.R. 2002. Metastasis to bone: causes, consequences and therapeutic opportunities. *Nat Rev Cancer* 2:584-593.
9. Thalmann, G.N., Anezinis, P.E., Chang, S.M., Zhou, H.E., Kim, E.E., Hopwood, V.L., Pathak, S., von Eschenbach, A.C., and Chung, L.W. 1994. Androgen-independent cancer progression and bone metastasis in the LNCaP model of human prostate cancer. *Cancer Res* 54:2577-2581.
10. Shevrin, D.H., Kukreja, S.C., Ghosh, L., and Lad, T.E. 1988. Development of skeletal metastasis by human prostate cancer in athymic nude mice. *Clin Exp Metastasis* 6:401-409.
11. Wu, T.T., Sikes, R.A., Cui, Q., Thalmann, G.N., Kao, C., Murphy, C.F., Yang, H., Zhou, H.E., Balian, G., and Chung, L.W. 1998. Establishing human prostate cancer cell xenografts in bone: induction of osteoblastic reaction by prostate-specific antigen-producing tumors in athymic and SCID/bg mice using LNCaP and lineage-derived metastatic sublines. *Int J Cancer* 77:887-894.
12. Ware, J.L., Paulson, D.F., Mickey, G.H., and Webb, K.S. 1982. Spontaneous metastasis of cells of the human prostate carcinoma cell line PC-3 in athymic nude mice. *J Urol* 128:1064-1067.
13. Paradis, V., Eschwege, P., Loric, S., Dumas, F., Ba, N., Benoit, G., Jardin, A., and Bedossa, P. 1998. De novo expression of CD44 in prostate carcinoma is correlated with systemic dissemination of prostate cancer. *J Clin Pathol* 51:798-802.
14. Desai, B., Rogers, M.J., and Chellaiah, M.A. 2007. Mechanisms of osteopontin and CD44 as metastatic principles in prostate cancer cells. *Molecular cancer* 6:18.

15. Slack, J.K., Adams, R.B., Rovin, J.D., Bissonette, E.A., Stoker, C.E., and Parsons, J.T. 2001. Alterations in the focal adhesion kinase/Src signal transduction pathway correlate with increased migratory capacity of prostate carcinoma cells. *Oncogene* 20:1152-1163.
16. Agoulnik, I.U., Vaid, A., Bingman, W.E., 3rd, Erdeme, H., Frolov, A., Smith, C.L., Ayala, G., Ittmann, M.M., and Weigel, N.L. 2005. Role of SRC-1 in the promotion of prostate cancer cell growth and tumor progression. *Cancer Res* 65:7959-7967.
17. Luangdilok, S., Box, C., Patterson, L., Court, W., Harrington, K., Pitkin, L., Rhys-Evans, P., O-charoenrat, P., and Eccles, S. 2007. Syk tyrosine kinase is linked to cell motility and progression in squamous cell carcinomas of the head and neck. *Cancer Research* 67:7907-7916.
18. Coopman, P.J., Do, M.T., Barth, M., Bowden, E.T., Hayes, A.J., Basyuk, E., Blancato, J.K., Vezza, P.R., McLeskey, S.W., Mangeat, P.H., et al. 2000. The Syk tyrosine kinase suppresses malignant growth of human breast cancer cells. *Nature* 406:742-747.
19. Truong, H.H., de Sonnevile, J., Ghotra, V.P., Xiong, J., Price, L., Hogendoorn, P.C., Spaink, H.H., van de Water, B., and Danen, E.H. 2012. Automated microinjection of cell-polymer suspensions in 3D ECM scaffolds for high-throughput quantitative cancer invasion screens. *Biomaterials* 33:181-188.
20. van Weerden, W.M., de Ridder, C.M., Verdaasdonk, C.L., Romijn, J.C., van der Kwast, T.H., Schroder, F.H., and van Steenbrugge, G.J. 1996. Development of seven new human prostate tumor xenograft models and their histopathological characterization. *Am J Pathol* 149:1055-1062.
21. Hahn, C.K., Berchuck, J.E., Ross, K.N., Kakoza, R.M., Clauser, K., Schinzel, A.C., Ross, L., Galinsky, I., Davis, T.N., Silver, S.J., et al. 2009. Proteomic and genetic approaches identify Syk as an AML target. *Cancer cell* 16:281-294.
22. Floryk, D., Tollaksen, S.L., Giometti, C.S., and Huberman, E. 2004. Differentiation of human prostate cancer PC-3 cells induced by inhibitors of inosine 5'-monophosphate dehydrogenase. *Cancer Res* 64:9049-9056.
23. Hall, C.L., Dubyk, C.W., Riesenberger, T.A., Shein, D., Keller, E.T., and van Golen, K.L. 2008. Type I collagen receptor (alpha2beta1) signaling promotes prostate cancer invasion through RhoC GTPase. *Neoplasia* 10:797-803.
24. Van Slambrouck, S., Hilken, J., Bisoffi, M., and Steelant, W.F. 2009. AsialoGM1 and integrin alpha2beta1 mediate prostate cancer progression. *Int J Oncol* 35:693-699.
25. Trerotola, M., Rathore, S., Goel, H.L., Li, J., Alberti, S., Piantelli, M., Adams, D., Jiang, Z., and Languino, L.R. CD133, Trop-2 and alpha2beta1 integrin surface receptors as markers of putative human prostate cancer stem cells. *Am J Transl Res* 2:135-144.
26. Fotheringham, J.A., Coalson, N.E., and Raab-Traub, N. Epstein-Barr Virus Latent Membrane Protein-2A Induces ITAM/Syk and Akt Dependent Epithelial Migration through alphaV-Integrin Membrane Translocation. *J Virol*.
27. Woollard, K.J., Fisch, C., Newby, R., and Griffiths, H.R. 2005. C-reactive protein mediates CD11b expression in monocytes through the non-receptor tyrosine kinase, Syk, and calcium mobilization but not through cytosolic peroxides. *Inflammation Research* 54:485-492.

28. Stoletov, K., Kato, H., Zardoujian, E., Kelber, J., Yang, J., Shattil, S., and Klemke, R. 2010. Visualizing extravasation dynamics of metastatic tumor cells. *J Cell Sci* 123:2332-2341.
29. Van den Hoogen, C., van der Horst, G., Cheung, H., Buijs, J.T., Pelger, R.C., and van der Pluijm, G. 2011. Integrin alpha_v expression is required for the acquisition of a metastatic stem/progenitor cell phenotype in human prostate cancer. *Am J Pathol* 179:2559-2568.
30. Baudot, A.D., Jeandel, P.Y., Mouska, X., Maurer, U., Tartare-Deckert, S., Raynaud, S.D., Cassuto, J.P., Ticchioni, M., and Deckert, M. 2009. The tyrosine kinase Syk regulates the survival of chronic lymphocytic leukemia B cells through PKCdelta and proteasome-dependent regulation of Mcl-1 expression. *Oncogene* 28:3261-3273.
31. Suljagic, M., Longo, P.G., Bennardo, S., Perlas, E., Leone, G., Laurenti, L., and Efremov, D.G. 2010. The Syk inhibitor fostamatinib disodium (R788) inhibits tumor growth in the Emu- TCL1 transgenic mouse model of CLL by blocking antigen-dependent B-cell receptor signaling. *Blood* 116:4894-4905.
32. Buchner, M., Baer, C., Prinz, G., Dierks, C., Burger, M., Zenz, T., Stilgenbauer, S., Jumaa, H., Veelken, H., and Zirlik, K. 2010. Spleen tyrosine kinase inhibition prevents chemokine- and integrin-mediated stromal protective effects in chronic lymphocytic leukemia. *Blood* 115:4497-4506.
33. Zhang, J., Benavente, C.A., McEvoy, J., Flores-Otero, J., Ding, L., Chen, X., Ulyanov, A., Wu, G., Wilson, M., Wang, J., et al. A novel retinoblastoma therapy from genomic and epigenetic analyses. *Nature* 481:329-334.
34. Zou, W., Reeve, J.L., Zhao, H., Ross, F.P., and Teitelbaum, S.L. 2009. Syk tyrosine 317 negatively regulates osteoclast function via the ubiquitin-protein isopeptide ligase activity of Cbl. *J Biol Chem* 284:18833-18839.
35. Yuan, Y., Mendez, R., Sahin, A., and Dai, J.L. 2001. Hypermethylation leads to silencing of the SYK gene in human breast cancer. *Cancer research* 61:5558-5561.
36. Wang, L., Duke, L., Zhang, P.S., Arlinghaus, R.B., Symmans, W.F., Sahin, A., Mendez, R., and Dai, J.L. 2003. Alternative splicing disrupts a nuclear localization signal in spleen tyrosine kinase that is required for invasion suppression in breast cancer. *Cancer research* 63:4724-4730.